International Journal of Pharmaceutics: X 4 (2022) 100129

Contents lists available at ScienceDirect

International Journal of Pharmaceutics: X

journal homepage: www.sciencedirect.com/journal/international-journal-of-pharmaceutics-x

Biological activity of gold nanoparticles combined with the NFL-TBS.40-63 peptide, or with other cell penetrating peptides, on rat glioblastoma cells

A. Griveau [a], C. Arib [b], J. Spadavecchia [b], J. Eyer [a,*]

[a] Univ Angers, Inserm, CNRS, MINT, SFR ICAT, F-49000 Angers, France
[b] CNRS, UMR 7244, CSPBAT, Laboratoire de Chimie, Structures et Propriétés de Biomatériaux Et D'Agents Thérapeutiques Université Paris 13, Sorbonne Paris Cité, Bobigny, France

ARTICLE INFO

Keywords:
Gold nanoparticles
BIOT-NFL-peptide
BIOT-Vim-peptide
BIOT-TAT-peptide
Transmission electron microscopy
Rat glioblastoma cells

ABSTRACT

Targeting, detecting, and destroying selectively cancer cells or specific organelles is a major challenge of nanomedicine. Recently, a new methodology was conceived to synthesize gold nanoparticles combined with a peptide having a C-terminal biotin (BIOT-NFL-peptide). This methodology called "Method IN" allows specific interactions between the BIOT-NFL-peptide, the polyethylene glycol diacid (PEG-COOH) and the gold salt (Au III) to produce multifunctional hybrid nano-carriers called BIOT-NFL-PEG-AuNPs. Here, we show that it is possible to use this strategy to synthesize multifunctional hybrid nano-carriers with other cell-penetrating peptides including TAT and Vim-peptides. *Ex-vivo* studies on F98 rat glioblastoma cells show that these new nanovectors acquire the cellular entry function of peptides and the gold particles make it possible to visualize by electron microscopy their localization in organelles. Thus, these new multifunctional nanovectors offer promising possibilities for the theranostic field, including the cell-penetrating property of the peptide, the intra-organelle localization of gold particles and their possible thermoplasmonic properties, as well as the stealth property of PEG.

1. Introduction

Glioblastoma (GBM) is the most frequent and aggressive cancer of the central nervous system and it is a diffuse and infiltrating tumor (Stupp et al., 2005). Current treatments are essentially palliative and consist of surgical excision associated with radio and/or chemotherapy (Stupp et al., 2005), but they are ineffective and toxic to healthy cells. Moreover, this treatment is regularly followed by recurrences due to the remaining stem cells which are particularly resistant to current treatments (Stupp et al., 2005). Therefore, it is essential to improve the specificity and the targeting of anti-GBM treatments.

Sequences capable of binding free tubulin are located along most of the intermediate filaments. They were identified mainly by peptide-array and called Tubulin Binding Sites (TBS) (Bocquet et al., 2009). A peptide corresponding to a sequence located on the light subunit of neurofilaments between the amino acids 40 and 63, called NFL-TBS.40–63 (for **N**euro **F**ilament **L**ow subunit **T**ubulin **B**inding **S**ite 40–63) or NFL-peptide, was further investigated. This peptide interacts specifically with different glioblastoma cell lines (mice, rats, human and canine) (Balzeau et al., 2013; Berges et al., 2012a; Griveau et al., 2021). It inhibits *in vitro* cell growth and *in vivo* tumor development (Berges et al., 2012a; Rivalin et al., 2014). The peptide alters the polymerization of microtubules in glioblastoma cells, without particularly affecting microtubules of healthy cells present in the nervous system (Berges et al., 2012a; Fressinaud and Eyer, 2014, 2015). The selective and massive internalization of the NFL-peptide in GBM cells occurs essentially by endocytosis, and no receptor has yet been identified (Lepinoux-Chambaud and Eyer, 2013). Using homology modeling it has been proposed that the binding of this peptide to a unique site of the C-terminal domain of the βIII-tubulin present in GBM cells could explain the

Abbreviations: GBM, Glioblastoma; TBS, Tubulin Binding Sites; NFL-peptide, NFL-TBS.40-63, or Neuro Filament Low subunit Tubulin Binding Site 40-63; Vim-peptide, Vim-TBS.58-81, or Vimentin Tubulin Binding Site 58-81; CPP, Cell-penetrating peptides; AuNPs, Gold nanoparticles; PEG-AuNPs, Polyethylene glycol gold nanoparticles; BIOT-CPP-PEG-AuNPs, Biotinylated cell-penetrating peptides polyethylene glycol gold nanoparticles; BIOT-NFL-PEG-AuNPs, Biotinylated NFL-peptide polyethylene glycol gold nanoparticles; BIOT-Vim-PEG-AuNPs, Biotinylated Vim-peptide polyethylene glycol gold nanoparticles; BIOT-TAT-PEG-AuNPs, Biotinylated TAT-peptide polyethylene glycol gold nanoparticles; TEM, Transmission electron microscopy.

* Corresponding author.
E-mail address: joel.eyer@univ-angers.fr (J. Eyer).

https://doi.org/10.1016/j.ijpx.2022.100129
Received 5 September 2022; Accepted 6 September 2022
Available online 16 September 2022

destruction of the microtubule network in these cells (Laurin et al., 2017, 2015). Taken together, these results show that the NFL-peptide represents a promising candidate for targeting glioblastoma cells. Other cell-penetrating peptides (CPP) derived from the intermediate filament Vimentin (Vim-TBS.58–81 (Vim)) (Balzeau et al., 2012; Bocquet et al., 2009) and the TAT.48–60-peptide (TAT) were also evaluated. In 1997, the TAT-peptide was identified as a peptide that can enter in cells (Vivès et al., 1997). Then, several studies showed that TAT-peptide can enter in the nuclei of glioma cells (Baker et al., 2007; Darbinian et al., 2001; Lo and Wang, 2008). The Vim-TBS.58–81 peptide crosses the plasma membrane, can enter in the nuclei of GBM cells, and thus can be an effective peptide vector in GBM cells (Balzeau et al., 2012). In this context, we were interested to develop new nanovectors based on these CPP-peptides.

The nanotechnologies development in the medical field knows very significant growth in the last decade. However, the nanoparticles development for therapeutic or diagnostic remains a challenge given the complexity of the expected objectives. Currently, there are many types of nanoparticles (Shapira et al., 2011) of different shapes that can be used, for example: micelles (Malmsten and Lindman, 1992), lipid nanoparticles: such as liposomes (Schnyder et al., 2005), lipid nanocapsules (Heurtault et al., 2002), solid nanoparticles (Lazăr et al., 2019), polymeric nanoparticles (Kreuter, 2004), or metallic nanoparticles (Zhu et al., 2017). Gold nanoparticles (AuNPs) are frequently used for their biocompatibility, their synthetic versatility, their electronic and optical properties (Her et al., 2017). Moreover, AuNPs can be used in photothermal therapy, and thanks the strong surface plasmon resonance effect, the resonant oscillation of free electrons takes place (Huang et al., 2006). The choice of gold nanoparticles is crucial in hyperthermia study and as tracker in high magnification imaging systems because this is not possible without gold nanoparticles. We have recently described the synthesis and physicochemical properties of such nanoparticles, in particular their thermoplasmonic properties (Arib et al., 2022). Several biomolecules, such as polymers, proteins, antibodies, or aptamers, were chelated with the gold salt and then encapsulated with the polymer to improve their stability and biocompatibility (Liu et al., 2020; Monteil et al., 2018; Moustaoui et al., 2016). Recently we developed such a methodology to Biotinylated-NFL-peptide (BIOT-NFL). Briefly, both the (PEG-$(COOH)_2$) and the BIOT-NFL-peptide participate to the growth and stabilization of gold-nanoparticles *via* complexation method (Method IN) through an electrostatic interaction between the chetone and amino groups of peptides and chloride auric ions in the mixture (Arib et al., 2022).

In this study, we extended this new strategy to other peptides including TAT or Vim-peptides and focused our attention on the *ex vivo* effects of such gold nanoparticles composed by BIOT-CPP-peptides (NFL, TAT, or Vim-peptides) and biocompatible polymer (PEG-$(COOH)_2$) on rat glioblastoma cells (F98 cells). We evaluated the efficiency of the combination between PEG-AuNPs alone and the BIOT-CPP-peptides on mitochondrial activity and whether the BIOT-CPP-PEG-AuNPs can internalize into F98 cells. For mitochondrial activity test, we used Colchicine as a positive control drug because this molecule, like the NFL-peptide, is well known to interact with tubulin, destroying the microtubule network and inducing cellular death (Bhattacharyya et al., 2008). Using electron microscopy, we were able to localize these functionalized gold particles in vacuoles of GBM cells. The development of these new multifunctional nanovectors offers promising possibilities for the theranostic field, in particular the cell-penetrating property of the peptide, the intra-organelle localization of gold particles and their possible thermoplasmonic properties, as well as the stealth property of PEG.

2. Material et methods

2.1. Reagent

The biotinylated NFL-TBS.40–63 peptide (NH_2-YSSY-SAPVSSSLSVRRSYSSSSGS-$CONH_2$), also called BIOT-NFL-peptide, was synthesized by PolyPeptide Group (Strasbourg, France). The biotinylated TAT.48–60 peptide (BIOT-TAT-peptide; BIOT-GRKKRRQRRRPPQ-$CONH_2$) and the biotinylated Vim-TBS.58–81 peptide (BIOT-Vim-peptide; BIOT-GGAYVTRSSAVRLRSSVPGVRLLQ-$CONH_2$) were synthetized by Millegen (Toulouse, France). Colchicine (1 µg/mL, C9754) has been purchased from Sigma-Aldrich (Saint Quentin Fallavier, France).

2.2. Synthesis and characterization of gold nanoparticles coupled with the BIOT-CPP-peptide (BIOT-CPP-PEG-AuNPs)

The PEG-AuNPs synthesis was based on the chemical reduction process described previously (Spadavecchia et al., 2016). Briefly, to combine CPP-peptides with PEG-AuNPs, tetrachloroauric acid ($HAuCl_4$, 1 mmol/L; Sigma-Aldrich) was added to BIOT-CCP-peptide and stirred for 10 min. After, a stabilizing agent, dicarboxylic polyethylene glycol-600 (PEG-$(COOH)_2$); Sigma-Aldrich) was added, and then sodium borohydride ($NaBH_4$, Sigma-Aldrich) was added. All details of synthesis, purification and characterization have been described previously (Arib et al., 2022). To confirm and characterize BIOT-CPP-PEG-AuNPs, several physicochemical techniques were used, including UV–visible spectroscopy, Raman spectroscopy, size and zeta potential measurements, and transmission electron microscopy, as previously described (Arib et al., 2022).

2.3. Transmission electron microscopy (TEM)

PEG-AuNPs, BIOT-NFL-PEG-AuNPs, BIOT-TAT-PEG-AuNPs, and BIOT-Vim-PEG-AuNPs were observed by transmission electron microscopy (TEM) at the Service Commun d'Imageries et d'Analyses Microscopiques (SCIAM; University of Angers, France). A 2 µL of each sample at 500 µmol/L of BIOT-CPP-PEG-AuNPs was deposited on copper grids (150 mesh) and stained with 2% uranyl acetate for one minute, and then dried under room temperature before observation. The examination was performed using a 120 kV electron microscope (Jeol, Japan) model JEM-1400, equipped with a Gatan SC1000 ORIUS® CCD camera (11 Megapixel) from USA. Gold nanoparticles are clearly visible in TEM and their nanometric size is evident on the electron micrographs. The contrasting agent (uranyl acetate) is used only to better reveal by transmission electron microscopy (TEM) the various organelles present in cells including the vesicles, the membrane, and the nucleus.

2.4. Mitochondrial activity

F98 rat glioblastoma cells were cultured in Dulbecco's modified Eagle's medium (DMEM; Sigma-Aldrich) containing GlutaMax and supplemented with 10% of fetal bovine serum (Sigma-Aldrich), 1% of antibiotics (100× streptomycin/penicillin; BioWest, Nuaille, France) and 1% of non-essential amino acids (Sigma-Aldrich). F98 cells were seeded in 96-well plates at 3000 or 1000 cells per well and incubated for 24 h at 37 °C and 5% CO_2. Then, the culture media was removed and Colchicine (1 µg/mL, Sigma-Aldrich), PEG-AuNPs, BIOT-NFL-PEG-AuNPs, BIOT-TAT-PEG-AuNPs, or BIOT-Vim-PEG-AuNPs at different concentrations (0, 50, 100, 250, 500 or 1000 µmol/L of BIOT-CPP-PEG-AuNPs) in fresh media, were tested for 24 or 72 h at 37 °C and 5% CO_2. Then, the MTS survival assay (ab197010; Abcam, Paris, France) was used to quantify the mitochondrial activity. Briefly, 20 µL of MTS reagent was added to each well for 4 h; the number of living cells is directly proportional to the absorbance measured by the amount of light absorbance at 490 nm in a SpectraMax M2 multi-scanning

spectrophotometer (Molecular Devices, San Jose, California, USA).

2.5. Analysis of cellular internalization by transmission electron microscopy

F98 cells were seeded in 12-well plates at 100,000 cells per well and were incubated for 24 h at 37 °C and 5% CO_2. Then, PEG-AuNPs, or BIOT-NFL-PEG-AuNPs at 500 µmol/L were incubated for 72 h. BIOT-TAT-PEG-AuNPs, or BIOT-Vim-PEG-AuNPs at 250 µmol/L were incubated for 24 h. The choice of the concentration and the incubation time was realized according to the results obtained on mitochondrial activity. After incubation, cells were washed with 0.1 M phosphate buffer at pH 7.4 and were fixed with a solution of 2.5% glutaraldehyde in 0.1 M phosphate buffer, overnight at 4 °C. The next day, the fixator was removed, and cells were rinsed with 0.1 M phosphate buffer. Then, cells were rinsed with distilled water and post-fixed with a solution of 1% osmium tetroxide in water for 1 h. Then, cells were rinsed with water (3 times 5 min) and incubated 15 min in 50° ethanol, 15 min in 70° ethanol, 15 min in 95° ethanol and 3 times 30 min in 100° ethanol. The cells were placed in a solution of 50% 100° ethanol and 50% Epon resin mixture (*v*/v) overnight. The next day, the Epon mixture was removed and replaced by a pure Epon bath for 4 h, then this bath was replaced by another pure Epon bath 24 h at 37 °C, then 24 h at 45 °C and 72 h at 60 °C. When the resin has polymerized at 60 °C, ultra-fine sections 60 nm thick were made with a UC7 ultramicrotome (Leica, Wetzlar, Germany) and deposited on 150 mesh copper grids. The sections were contrasted with a solution of 3% uranyl acetate in 50° ethanol for 15 min then rinsed with ultrapure water. Samples were observed using a 120 kV Jeol JEM-1400 electron microscope (Japan) with a SC1000 Orius model 832 (Gatan) 4 k CCD camera.

2.6. Statistical analysis

All data are represented as mean ± SEM. All experiments are repeated at least three times. Statistical analyzes were performed using GraphPad Prism 7.03 (GraphPad software, San Diego, USA). The asterisks indicate significant level *p < 0.05; **p < 0.005 and ***p < 0.001.

3. Results

3.1. Synthesis of BIOT-CPP-PEG-AuNPs

Fig. 1 displays a schematic representation of BIOT-CPP-PEG-AuNPs synthesis, with BIOT-NFL-peptide as example. This methodology (Method IN) has already been developed and published with different drugs/biomolecules (Arib et al., 2021a, 2021b; Barbey et al., 2021; Moustaoui et al., 2016; Song et al., 2020). In the present paper, we applied BIOT-CPP-peptides, as biomolecules of interest to build a specific nanovector. For this aim, three steps are necessary in the synthesis: 1) complexation between $HAuCl_4$ and BIOT-CPP-peptide, 2) pegylation with dicarboxylic polyethylene glycol-600 (PEG-$(COOH)_2$) to form $HAuCl_4$/BIOT-CPP-peptide complex, and finally 3) reduction with-sodium borohydride ($NaBH_4$) to obtain the final product. All BIOT-CPP-PEG-AuNPs were characterized by spectroscopic techniques before testing their effects on GBM cells (Arib et al., 2022). With the UV–Vis spectra and the Raman spectra, we have confirmed the complexation between BIOT-CPPs and PEG-AuNPs (Arib et al., 2022). It was also used to determine the amount of peptide present in such particles and this was our reference for quantification of the particles. Using the Zetasizer, the mean size for respectively PEG-AuNPs, BIOT-NFL-PEG-AuNPs, BIOT-TAT-PEG-AuNPs, and BIOT-Vim-PEG-AuNPs was 25 ± 2 nm, 91 ± 2 nm, 104 ± 2 nm, and 101 ± 2 nm. The measures of the zeta potential are negative, −24 ± 0.2 mV, −29 ± 0.6 mV, and − 33 ± 0.8 mV for respectively PEG-AuNPs, BIOT-TAT-PEG-AuNPs, and BIOT-Vim-PEG-AuNPs; and positive for BIOT-NFL-PEG-AuNPs (+24 ± 0.7 mV) (Arib et al., 2022).

3.2. The combination between the BIOT-NFL-peptide and PEG-AuNPs modifies the structure of nanoparticles

The first experiment was focused on the analysis of BIOT-CPP-PEG-AuNPs morphology at 500 µmol/L by transmission electron microscope (TEM). We observed a difference of the ultrastructure of the nanoparticles formed with and without the BIOT-NFL-peptide. As shown in Fig. 2A, PEG-AuNPs nanoparticles have a round shape with relatively homogeneous sizes of 12.25 ± 1.28 nm. When the BIOT-NFL-peptide

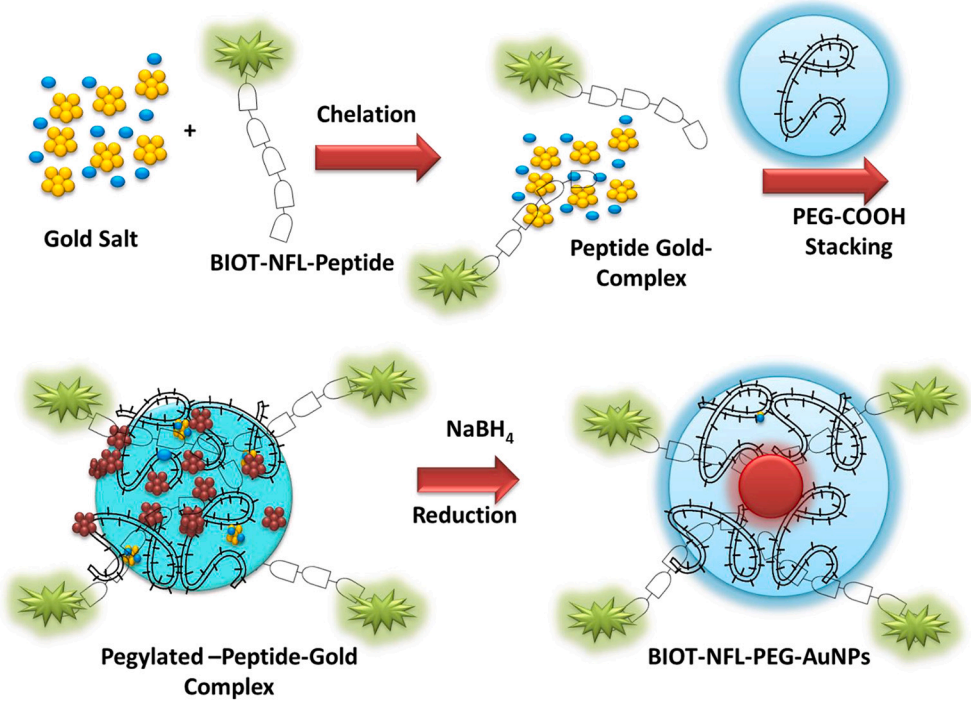

Fig. 1. Schematic representation of synthesis of gold nanoparticles combined with the BIOT-NFL-peptide (BIOT-NFL-PEG-AuNPs). As described in Arib et al., 2022, a complex between tetrachloroauric acid ($HAuCl_4$) with BIOT-NFL-peptide was created. Then, a stabilizing agent, dicarboxylic polyethylene glycol-600 (PEG$(COOH)_2$), and sodium borohydride ($NaBH_4$) were added. Finally, BIOT-NFL-PEG-AuNPs were synthetized. The same process was used for BIOT-TAT-PEG-AuNPs, and BIOT-Vim-PEG-AuNPs. (For interpretation of the references to colour in this figure legend, the reader is referred to the web version of this article.)

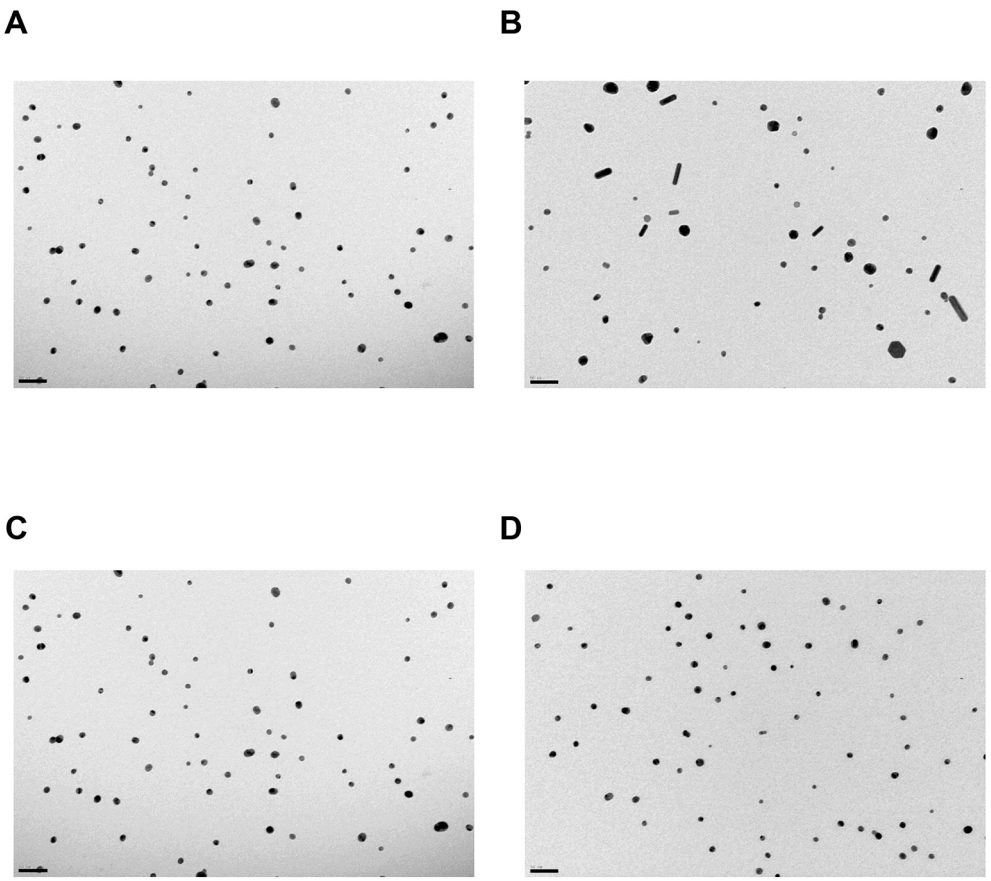

Fig. 2. Characterization of gold nanoparticles (PEG-AuNPs) combined or not with the BIOT-CPP-peptide by transmission electron microscopy (TEM). **(A)** TEM images of PEG-AuNPs, **(B)** of BIOT-NFL-PEG-AuNPs, **(C)** of BIOT-TAT-PEG-AuNPs, and **(D)** of BIOT-Vim-PEG-AuNPs. Scale bars: 50 nm. (For interpretation of the references to colour in this figure legend, the reader is referred to the web version of this article.)

was complexed with pegylated gold salt, to form BIOT-NFL-PEG-AuNPs, we observed several particle shapes (round, rod, hexagon) with quite heterogeneous sizes (Fig. 2B). We observed long rods with a maximum length around 50 nm. In contrast, the combination of the TAT-peptide (Fig. 2C) or the Vim-peptide (Fig. 2D) with pegylated gold salt to form corresponding Vim/TAT-peptide gold nanoparticles did not dramatically change the morphology of nanoparticles. The size mean was 27.25 ± 8.97 nm, and 34.86 ± 9.94 nm for respectively BIOT-TAT-PEG-AuNPs (Fig. 2C), and BIOT-Vim-PEG-AuNPs (Fig. 2D).

3.3. PEG-AuNPs combined with BIOT-CCP-peptides decrease mitochondrial activity of rat glioblastoma cells

BIOT-CPP-PEG-AuNPs were tested on rat glioblastoma cells (F98), and the mitochondrial activity was measured. F98 cells were treated with a range of concentrations of BIOT-CPP-PEG-AuNPs (between 0 and 1000 µmol/L) for 24 or 72 h, and a MTS assay was performed. Colchicine (Col, 1 µg/mL), a positive control was used, because like the NFL-peptide this drug interacts with tubulin, disturbing the assembly of microtubules and inducing cellular death (Bhattacharyya et al., 2008). With a 24-h treatment, PEG-AuNPs regardless of the concentration used have no detectable impact on mitochondrial activity, while BIOT-NFL-PEG-AuNPs at 1000 µmol/L decrease mitochondrial activity (Fig. 3A). When the treatment time was increased (72 h), PEG-AuNPs decreased mitochondrial activity by about 30%, but BIOT-NFL-PEG-AuNPs decreased it more (Fig. 3B). At 1000 µmol/L of PEG-AuNPs, the mitochondrial activity is 69.70 ± 0.04%, and 13.00 ± 0.03% with the BIOT-NFL-PEG-AuNPs treatment.

The same experiments were performed with BIOT-TAT-PEG-AuNPs, and BIOT-Vim-PEG-AuNPs on F98 cells (Fig. 4A-B). Significant toxicity was observed with BIOT-TAT-PEG-AuNPs, all cells died with treatment at 500 and 1000 µmol/L for 24 or 72 h (Fig. 4A-B). We observed the same results concerning PEG-AuNPs, no toxicity with a treatment for 24 h (Fig. 4A), and a small decrease of mitochondrial activity with a 72-h treatment (Fig. 4B). For 72 h-treatment, a similar decrease of mitochondrial activity was observed with PEG-AuNPs at 1000 µmol/L, BIOT-TAT-PEG-AuNPs at 250 µmol/L, and BIOT-Vim-PEG-AuNPs at 500 µmol/L, respectively 68.08 ± 0.04%, 71.44 ± 0.14%, and 68.19 ± 0.13% (Fig. 4B). For the three BIOT-CPP-peptides, the combination with PEG-AuNPs has no impact on the biological activity of CPP-peptides and does not alter the CPP-peptide function.

3.4. BIOT-CPP-PEG-AuNPs increase cellular internalization and have an impact on cellular morphology

We further investigated the capacity of BIOT-CPP-PEG-AuNPs to internalize in the rat GBM cells by transmission electron microscopy (TEM). F98 cells were treated with PEG-AuNPs, or BIOT-NFL-PEG-AuNPs at 500 µmol/L for 72 h. We chose this concentration based on the results obtained on mitochondrial activity; at 500 µmol/L a decrease was observed with BIOT-NFL-PEG-AuNPs (Fig. 3B). Fig. 5A represents TEM images of non-treated F98 cells presenting normal nucleus (N) as well as classical cellular extensions. F98 cells treated with PEG-AuNPs present few nanoparticles in cellular vacuoles (Fig. 5B and Supplemental Fig. 1). When GBM cells were treated with BIOT-NFL-PEG-AuNPs, more nanoparticles into the cells and more cellular vacuoles (V) were observed, and the cellular extension are shorter (Fig. 5C and Supplemental Fig. 2). We observed heterogeneity in size and shape of

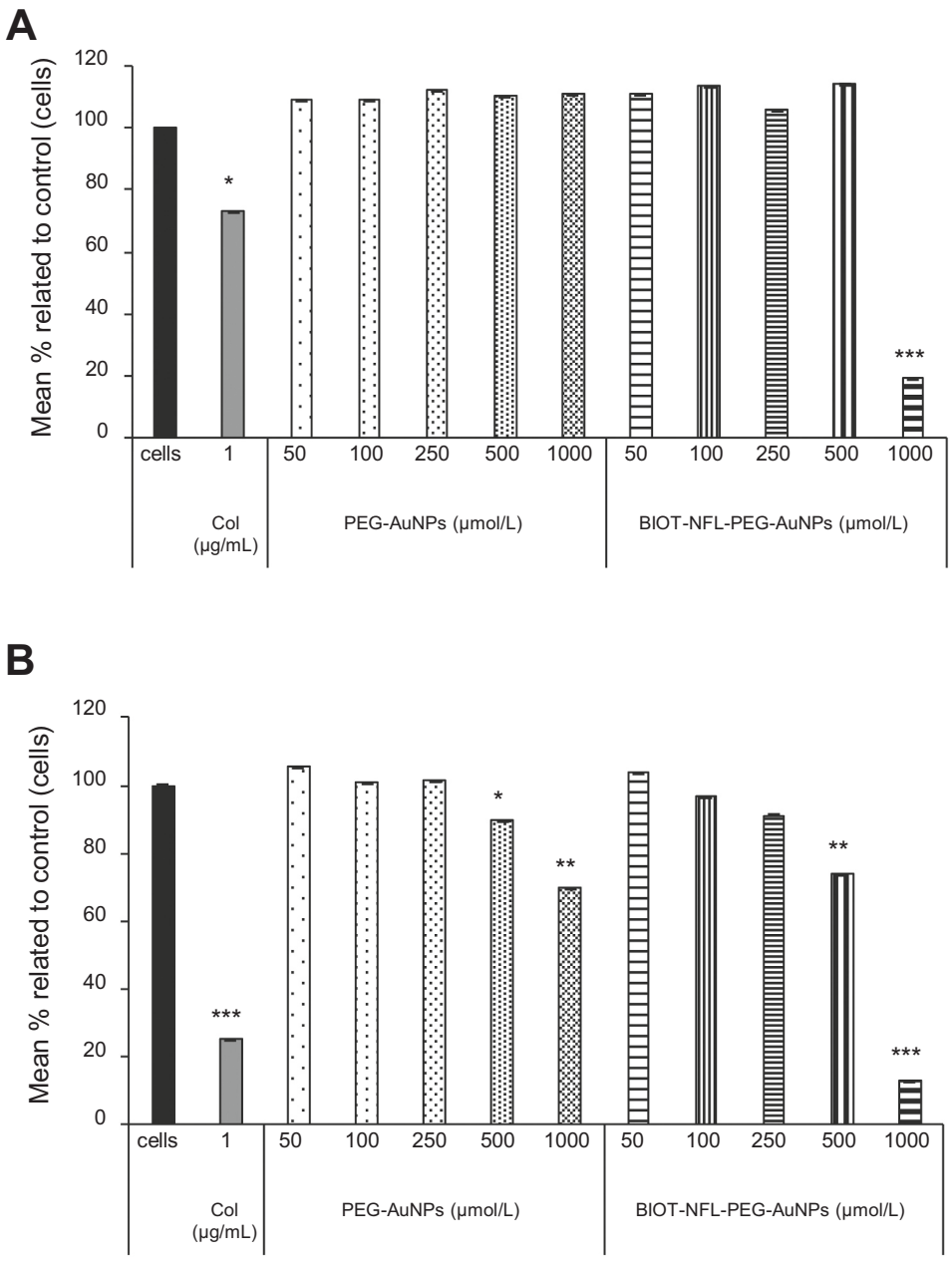

Fig. 3. *In vitro* effects of gold nanoparticles (PEG-AuNPs) alone, or with the BIOT-NFL-peptide (BIOT-NFL-PEG-AuNPs) on rat glioblastoma cells (F98) mitochondrial activity. F98 cells were treated with nanoparticles alone, with the BIOT-NFL-PEG-AuNPs at 0, 50, 100, 250, 500 or 1000 µmol/L; or with the positive control Colchicine (Col, 1 µg/mL), for 24 h **(A)** or 72 h **(B)**. Then, the mitochondrial activity was evaluated by MTS assay. Experiments were performed at least in triplicate. Data are represented as mean ± SEM. Statistical analysis was performed with Student's *t*-test (*p < 0.05; **p < 0.005 and ***p < 0.001). (For interpretation of the references to colour in this figure legend, the reader is referred to the web version of this article.)

BIOT-NFL-PEG-AuNPs nanoparticles in GBM cells.

We also investigated BIOT-TAT-PEG-AuNPs, and BIOT-Vim-PEG-AuNPs. F98 cells were treated with BIOT-TAT-PEG-AuNPs, or BIOT-Vim-PEG-AuNPs at 250 µmol/L for 24 h. Results on mitochondrial activity showed a strong effect of BIOT-TAT-PEG-AuNPs (Fig. 4), and we decided to treat cells for 24 h at 250 µmol/L of nanoparticles. Fig. 6A represents TEM images of F98 cells treated with PEG-AuNPs at 250 µmol/L with few nanoparticles. When PEG-AuNPs are combined with the TAT- (Fig. 6B) or the Vim-peptide (Fig. 6C), then incubated with cells, the nanoparticles morphology changed, and more cellular vacuoles are detected. The amount of PEG-AuNPs, or BIOT-CPP-PEG-AuNPs was quantified by manual counting the particles on the electron micrographs and were presented in Supplemental Fig. 3.

In Fig. 7, we observed nanoparticles morphology after incubation with the GBM cells. BIOT-NFL-PEG-AuNPs showed similar morphology in solution (Fig. 2B) or in cells (Fig. 7B), with heterogeneous sizes and shapes. Concerning BIOT-TAT (Fig. 7C), or BIOT-Vim-PEG-AuNPs (Fig. 7D), a notable change of morphology was observed. In solution, the nanoparticles are ovals (Fig. 1C–D), and when they were incubated with the GBM cells, the nanoparticles are in the form of balls (Fig. 7C–D). It should be noted that during the synthesis, the quantity of CPP is not the same. Indeed, to optimize the stability of the nanoparticles, the quantity of TAT and Vim-peptides was reduced by two (Arib et al., 2022).

4. Discussion

In this study, a novel type of nanoparticles composed of nanogold particles (AuNPs), polyethylene glycol-600 (PEG), and BIOT-CPP-peptides (NFL, TAT, or Vim-peptides) was synthetized and investigated. As detailed previously for the NFL-peptide (Arib et al., 2022), the production of such nanoparticles is particularly robust and is working very well with all the peptides tested so far (Fig. 1). This strategy allows to conserve the targeting and cellular internalization properties of the

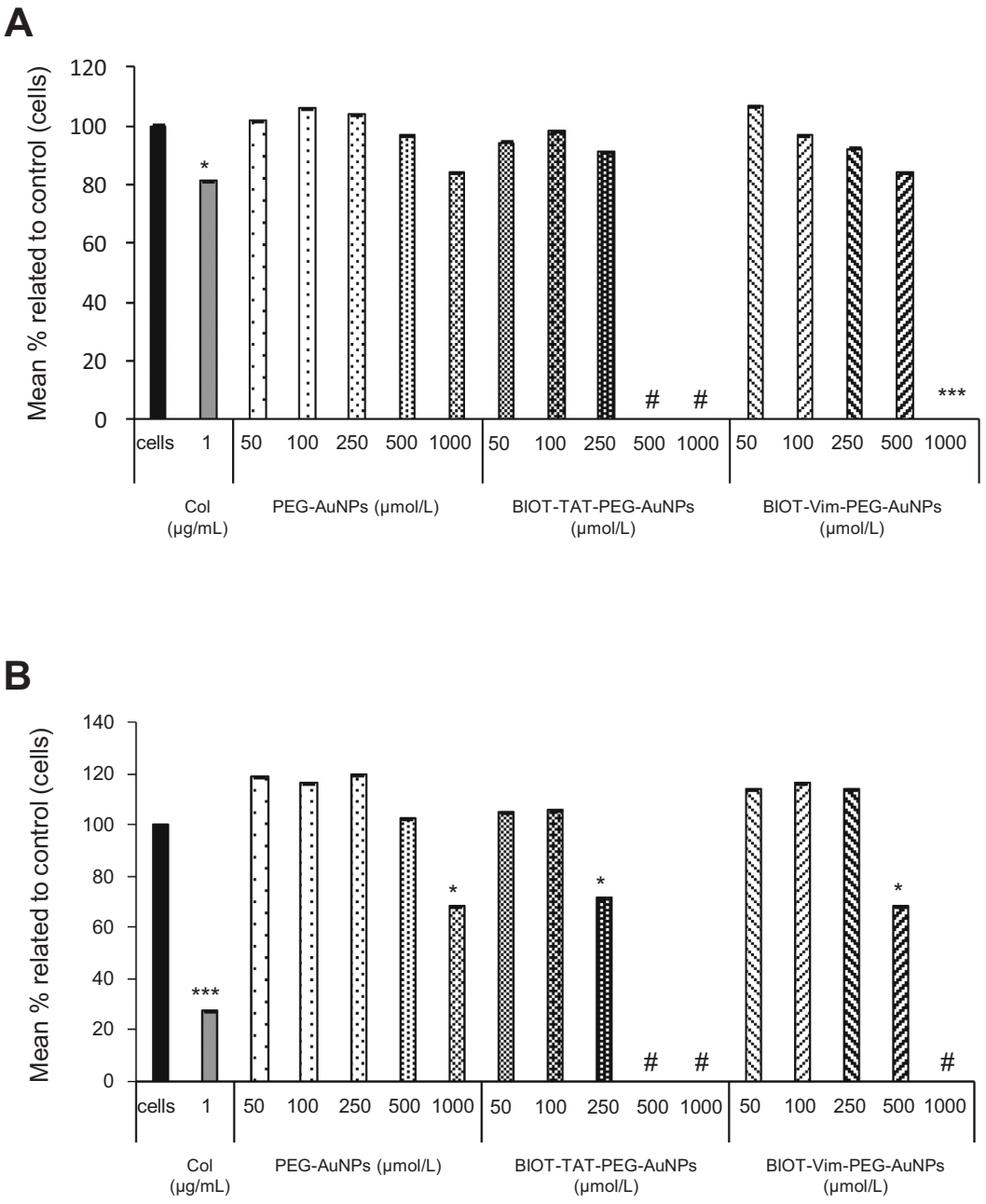

Fig. 4. *In vitro* effects of gold nanoparticles (PEG-AuNPs) alone, or with the BIOT-TAT-peptide (BIOT-TAT-PEG-AuNPs), or with the BIOT-Vim-peptide (BIOT-Vim-PEG-AuNPs) on rat glioblastoma cells (F98) mitochondrial activity. F98 cells were treated with nanoparticles alone, with the different CPP-PEG-AuNPs nanoparticles at 0, 50, 100, 250, 500 or 1000 µmol/L; or with the positive control Colchicine (Col, 1 µg/mL), for 24 h **(A)** or 72 h **(B)**. Then, the mitochondrial activity was evaluated by MTS assay. Experiments were performed at least in triplicate. # No cells are present at the end of the treatment incubation. Data are represented as mean ± SEM. Statistical analysis was performed with Student's t-test (*$p < 0.05$ and ***$p < 0.001$). (For interpretation of the references to colour in this figure legend, the reader is referred to the web version of this article.)

tested peptides for a long period of time (6 to 12 months), and thus represents a very useful strategy to develop new type of nanoparticles.

To characterize these BIOT-CPP-PEG-AuNPs, several observations with transmission electron microscopy (TEM) were performed (Fig. 2). A major difference was observed with the BIOT-NFL-peptide, and the combination between this peptide and PEG-AuNPs changed the particles morphology and polydisperse nanoparticles were observed (Fig. 2B). With the TAT-peptide (Fig. 2C), or with the Vim-peptide (Fig. 2D), no major morphology or size difference was observed. Therefore, these results indicate that the morphology changes are not due to the presence of Biotin but is a specific characteristic of the peptide complex, thanks to a different steric arrangement of the peptide under chelation with gold salt. Another possible explanation would be that the conformation of the peptides changes according to the medium used, as has been shown for the NFL-peptide (alpha helices or beta sheets) (Berges et al., 2012b). Previously other authors have demonstrated that the shape of nanoparticles combined with CPP is dependent on the CPP sequence used (Margus et al., 2016). Moreover, during the synthesis, the peptide quantity (TAT, or Vim-peptides) was reduced by two to allow a better stability, and this difference could explain the difference of nanoparticle morphology (Arib et al., 2022).

Then, we studied the properties of nanoparticles composed of BIOT-

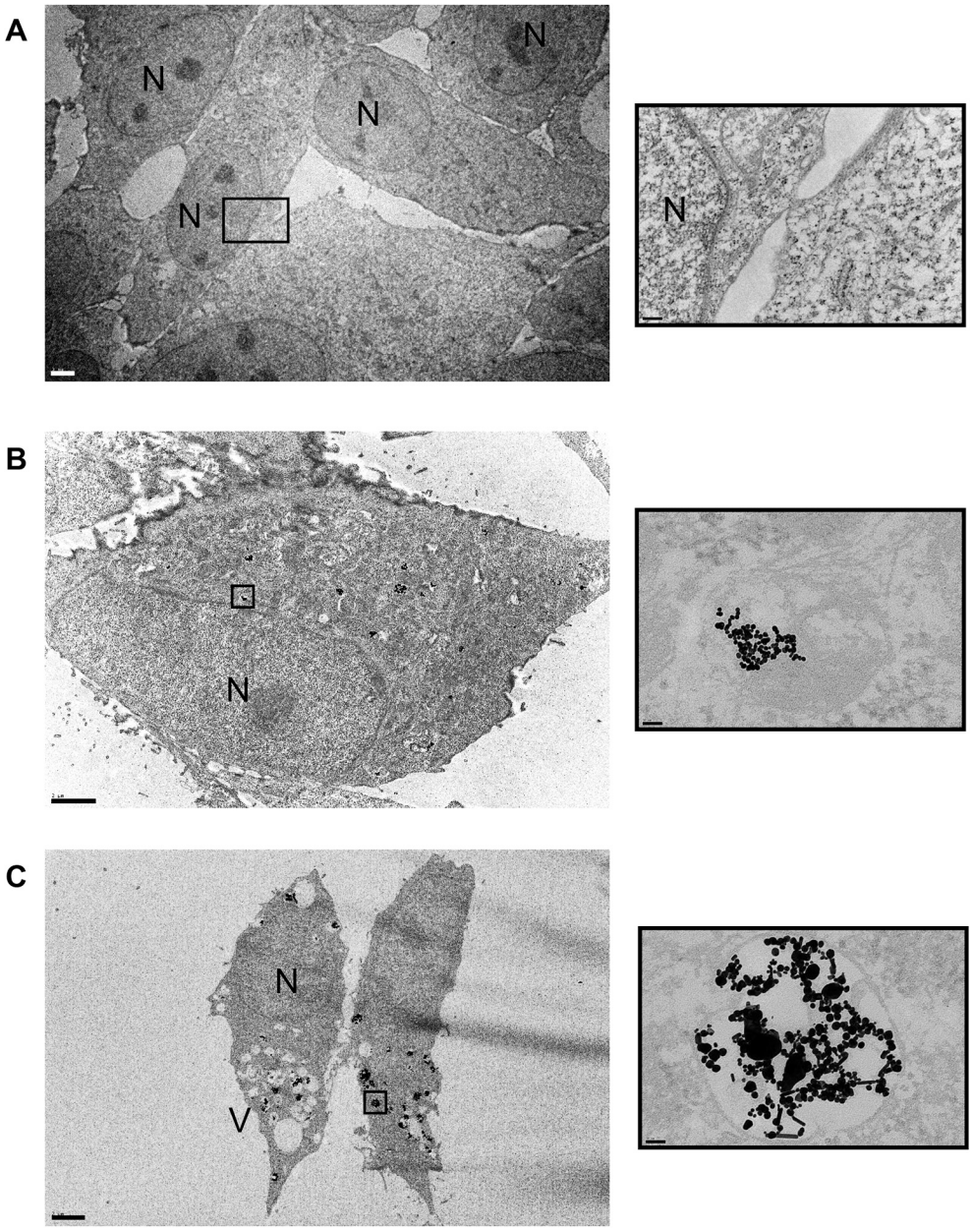

Fig. 5. Transmission electron microscope images illustrating the internalization of gold nanoparticles (PEG-AuNPs) alone or coupled with the BIOT-NFL-peptide (BIOT-NFL-PEG-AuNPs) in rat glioblastoma cells. F98 cells were treated with nanoparticles at 500 µmol/L for 72 h. Cells were observed with a TEM. **(A)** Control F98 cells (no treatment), **(B)** F98 cells treated with PEG-AuNPs, and **(C)** F98 cells treated with BIOT-NFL-PEG-AuNPs. N for nucleus and V for vacuoles. Scale bars (at left): 2 µm. Scale bars (at right): 200 nm for A and 50 nm for B and C. (For interpretation of the references to colour in this figure legend, the reader is referred to the web version of this article.)

CPP-PEG-AuNPs on mitochondrial activity of rat glioblastoma cells (F98). We showed that at high concentration (1000 µmol/L) the BIOT-NFL-PEG-AuNPs reduces the mitochondrial activity of F98 cells (Fig. 3A), and this reduction is more important with the time of treatment (Fig. 3B). For the PEG-AuNPs, no toxicity was observed with 24 h of treatment (Fig. 3A and 4A) and a slight decrease of mitochondrial activity was observed for 72 h of treatment (Fig. 3B and 4B). Moreover, BIOT-NFL-PEG-AuNPs are stable at least 12 months (Arib et al., 2022), and the cellular biological activity of the BIOT-NFL-peptide is maintained. Although the addition of TAT, or Vim-peptide to PEG-AuNPs does not change the particle structure (Fig. 2C–D), an impact on mitochondrial activity was observed (Fig. 4). The effect on the mitochondrial activity is very high, because with BIOT-TAT-PEG-AuNPs at 500 and 1000 µmol/L, all GBM cells died regardless of treatment time (Fig. 4). The treatment with BIOT-Vim-PEG-AuNPs decreases mitochondrial activity at high concentration (Fig. 4). For the three BIOT-CPP-PEG-AuNPs, an impact on mitochondrial activity was observed, regardless of the shape of the particles. On glioma cells (A172), a combination between an angiogenin peptide and nanogold showed also a decrease of cell viability (Naletova et al., 2019). Similarly, a reduction of cell viability (U87MG) was observed when cells were treated with nanogold combined with RGD-peptide (Gao et al., 2020).

We also performed TEM experiments to analyze the cellular internalization of BIOT-CPP-PEG-AuNPs. We showed the efficiency of BIOT-CPP-PEG-AuNPs to be better internalized in F98 cells compared to PEG-AuNPs alone (Fig. 5 and 6). We also showed that the biological function of BIOT-CPP-peptides is not impacted by the combination with PEG-AuNPs, because we observed an effect on cellular morphology with a reduction of cellular extensions and the presence of more cellular vacuoles. The TAT-peptide is known for the capacity to enter in nucleus (Vivès et al., 1997), but when this peptide was associated with PEG-AuNPs, the nuclear translocation was not observed (Fig. 6B). However, some studies have shown a possible nuclear translocation of Au nanoparticles combined with the TAT-peptide (de la Fuente and Berry, 2005; Krpetić et al., 2011), but the strategy and the method of synthesis of nanoparticles as well as the cell type tested are different. Krpetić and

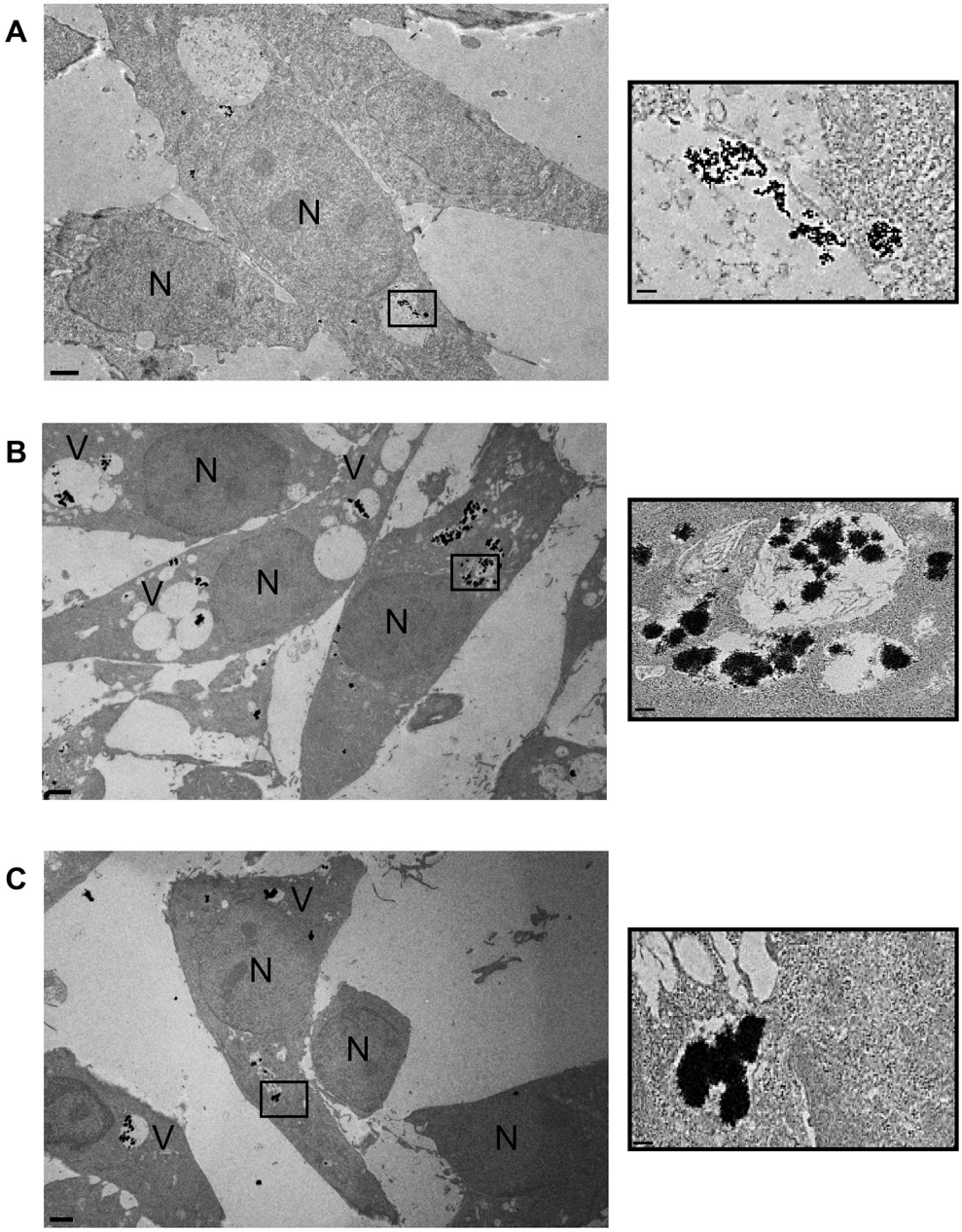

Fig. 6. Transmission electron microscope images illustrating the internalization of gold nanoparticles (PEG-AuNPs) alone, coupled with the BIOT-TAT-peptide (BIOT-TAT-PEG-AuNPs), or with the BIOT-Vim-peptide (BIOT-Vim-PEG-AuNPs) in rat glioblastoma cells. F98 cells were treated with nanoparticles at 250 µmol/L for 24 h. Cells were observed with a TEM. **(A)** F98 cells treated with PEG-AuNPs, **(B)** F98 cells treated with BIOT-TAT-PEG-AuNPs, and **(C)** F98 cells treated with BIOT-Vim-PEG-AuNPs. N for nucleus and V for vacuoles. Scale bars (at left): 2 µm. Scale bars (at right): 50 nm. (For interpretation of the references to colour in this figure legend, the reader is referred to the web version of this article.)

colleagues showed that the nuclear accumulation of AuNPs is not detectable after 24 h (Krpetić et al., 2011), and this paper could explain the no nuclear detection of BIOT-TAT-PEG-AuNPs after the GBM cell treatment for 24 h. The time-incubation seems to be an important parameter to visualize gold nanoparticles in the nucleus. We tried increasing the treatment time, but all the cells died, and it was impossible to perform TEM analysis.

We showed similar morphology for BIOT-NFL-PEG-AuNPs in solution (Fig. 2B) or in cells (Fig. 7B). But we observed a change in morphology in solution compared to cells for BIOT-TAT-PEG-AuNPs (Fig. 1C and 7C), and for BIOT-Vim-PEG-AuNPs (Fig. 1D and 7D). This change in morphology of gold particles is a process that has already been observed. Indeed, a team has shown the biotransformation of gold particles in primary human fibroblasts. This study highlighted the degradation of gold particles in lysosomes as well as a phenomenon of recrystallization and self-assembly of their degradation products (Balfourier et al., 2020). We may be in the presence of the same intracellular phenomenon with BIOT-TAT/Vim-PEG-AuNPs in GBM cells. To confirm this, it would be necessary to carry out transcriptomic analyzes to detect the gold particles as well as their degradation products.

5. Conclusion

This work demonstrates and confirms the possibility of synthesizing new multifunctional nanovectors composed of BIOT-CPP-peptides, and PEG-AuNPs. Three BIOT-CPP-peptides were used and tested on rat glioblastoma cells. For all BIOT-CPP-PEG-AuNPs, we demonstrated their better cellular internalization when combined to CPP-peptides, their intra-organelle localization, and their impact on mitochondrial activity. This system can be used with other cell penetrating peptides to target other cell types. It also offers interesting opportunities in the cancer therapeutic treatment, and other possible diseases. To summarize the promising prospects in the theranostic field, we can cite the property of targeting certain cells according to the peptide used, the intra-organelle localization of gold particles thanks to electron microscopy, the development of thermoplasmonic properties linked to gold particles and the

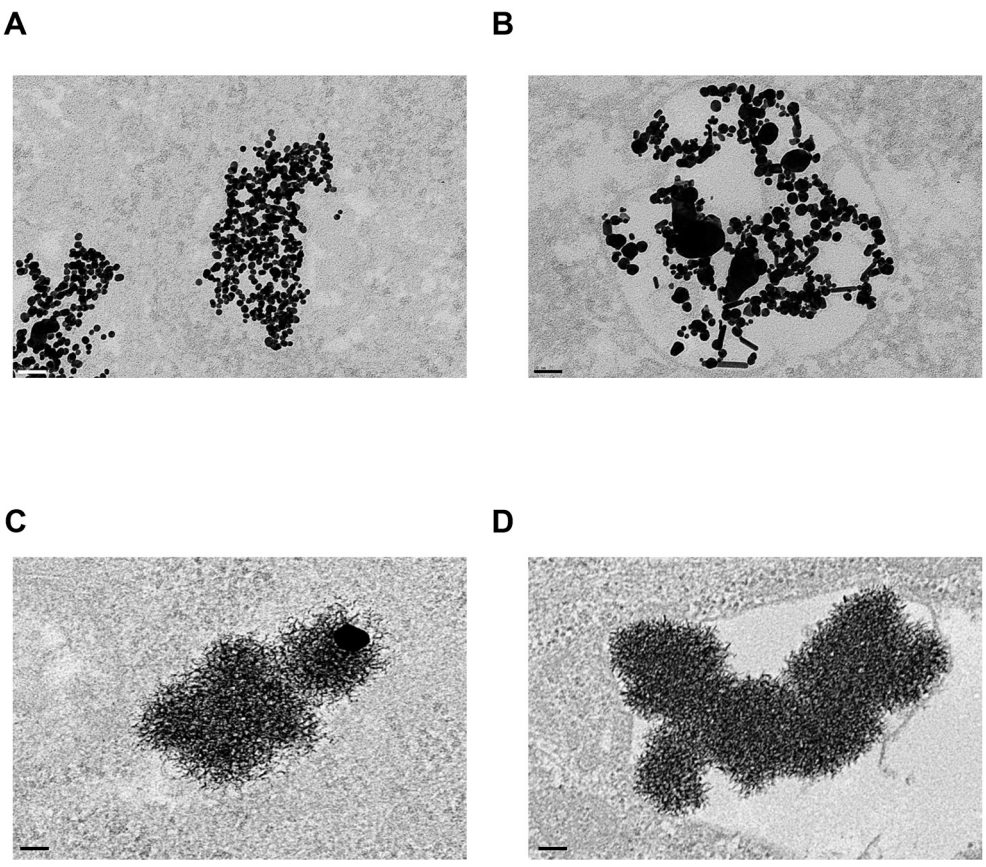

Fig. 7. Biological TEM images showing the morphology of PEG-AuNPs alone and combined with BIOT-CPP-peptides after F98 cells treatment. F98 cells were treated with 500 µmol/L of PEG-AuNPs **(A)**, or of BIOT-NFL-PEG-AuNPs **(B)** for 72 h. F98 cells were treated with 250 µmol/L of BIOT-TAT-PEG-AuNPs **(C)**, or of BIOT-Vim-PEG-AuNPs **(D)** for 24 h. Scale bars: 50 nm.

stealth provided by the PEG.

Funding

This work has been supported by "Ligue contre le Cancer 49", and "Plan Cancer Inserm"to Joël Eyer.

Declaration of Competing Interest

The authors declare that they have no conflict of interest, with respect to the research, authorship, and/or publication of this article.

Data availability

Data will be made available on request.

Acknowledgement

The authors acknowledge Florence Manero from SCIAM (Service Commun d'Imageries et d'Analyses Microscopiques, Angers) for microscopy analysis.

Appendix A. Supplementary data

Supplementary data to this article can be found online at https://doi.org/10.1016/j.ijpx.2022.100129.

References

Arib, C., Bouchemal, N., Barile, M., Paleni, D., Djaker, N., Dupont, N., Spadavecchia, J., 2021a. Flavin-adenine-dinucleotide gold complex nanoparticles: chemical modeling design, physico-chemical assessment and perspectives in nanomedicine. Nanoscale Adv. 3, 6144–6156. https://doi.org/10.1039/D1NA00444A.

Arib, C., Spadavecchia, J., de la Chapelle, M.L., 2021b. Enzyme mediated synthesis of hybrid polyedric gold nanoparticles. Sci. Rep. 11, 3208. https://doi.org/10.1038/s41598-021-81751-1.

Arib, C., Griveau, A., Eyer, J., Spadavecchia, J., 2022. Cell penetrating peptides (CPP) gold (III) - complex - bioconjugates: from chemical design to interaction with cancer cells for nanomedicine applications. Nanoscale Adv. https://doi.org/10.1039/D2NA00096B.

Baker, R.D., Howl, J., Nicholl, I.D., 2007. A sychnological cell penetrating peptide mimic of p21(WAF1/CIP1) is pro-apoptogenic. Peptides 28, 731–740. https://doi.org/10.1016/j.peptides.2006.12.013.

Balfourier, A., Luciani, N., Wang, G., Lelong, G., Ersen, O., Khelfa, A., Alloyeau, D., Gazeau, F., Carn, F., 2020. Unexpected intracellular biodegradation and recrystallization of gold nanoparticles. Proc. Natl. Acad. Sci. 117, 103–113. https://doi.org/10.1073/pnas.1911734116.

Balzeau, J., Peterson, A., Eyer, J., 2012. The vimentin-tubulin binding site peptide (Vim-TBS.58-81) crosses the plasma membrane and enters the nuclei of human glioma cells. Int. J. Pharm. 423, 77–83. https://doi.org/10.1016/j.ijpharm.2011.04.067.

Balzeau, J., Pinier, M., Berges, R., Saulnier, P., Benoit, J.P., Eyer, J., 2013. The effect of functionalizing lipid nanocapsules with NFL-TBS.40-63 peptide on their uptake by glioblastoma cells. Biomaterials 34, 3381–3389. https://doi.org/10.1016/j.biomaterials.2013.01.068.

Barbey, C., Bouchemal, N., Retailleau, P., Dupont, N., Spadavecchia, J., 2021. Idarubicin–gold complex: from crystal growth to gold nanoparticles. ACS Omega 6, 1235–1245. https://doi.org/10.1021/acsomega.0c04501.

Berges, R., Balzeau, J., Peterson, A.C., Eyer, J., 2012a. A tubulin binding peptide targets glioma cells disrupting their microtubules, blocking migration, and inducing apoptosis. Mol. Ther. 20, 1367–1377. https://doi.org/10.1038/mt.2012.45.

Berges, R., Balzeau, J., Takahashi, M., Prevost, C., Eyer, J., 2012b. Structure-function analysis of the glioma targeting NFL-TBS.40-63 peptide corresponding to the tubulin-binding site on the light neurofilament subunit. PLoS One 7, e49436. https://doi.org/10.1371/journal.pone.0049436.

Bhattacharyya, B., Panda, D., Gupta, S., Banerjee, M., 2008. Anti-mitotic activity of colchicine and the structural basis for its interaction with tubulin. Med. Res. Rev. 28, 155–183. https://doi.org/10.1002/med.20097.

Bocquet, A., Berges, R., Frank, R., Robert, P., Peterson, A.C., Eyer, J., 2009. Neurofilaments bind tubulin and modulate its polymerization. J. Neurosci. 29, 11043–11054. https://doi.org/10.1523/JNEUROSCI.1924-09.2009.

Darbinian, N., Gallia, G.L., King, J., Del Valle, L., Johnson, E.M., Khalili, K., 2001. Growth inhibition of glioblastoma cells by human Pur? J. Cell. Physiol. 189, 334–340. https://doi.org/10.1002/jcp.10029.

de la Fuente, J.M., Berry, C.C., 2005. Tat peptide as an efficient molecule to translocate gold nanoparticles into the cell nucleus. Bioconjug. Chem. 16, 1176–1180. https://doi.org/10.1021/bc050033+.

Fressinaud, C., Eyer, J., 2014. Neurofilament-tubulin binding site peptide NFL-TBS.40-63 increases the differentiation of oligodendrocytes in vitro and partially prevents them from lysophosphatidyl choline toxiciy. J. Neurosci. Res. 92, 243–253. https://doi.org/10.1002/jnr.23308.

Fressinaud, C., Eyer, J., 2015. Neurofilaments and NFL-TBS.40-63 peptide penetrate oligodendrocytes through clathrin-dependent endocytosis to promote their growth and survival in vitro. Neuroscience 298, 42–51. https://doi.org/10.1016/j.neuroscience.2015.04.003.

Gao, H., Chu, C., Cheng, Y., Zhang, Y., Pang, X., Li, D., Wang, X., Ren, E., Xie, F., Bai, Y., Chen, L., Liu, G., Wang, M., 2020. In situ formation of nanotheranostics to overcome the blood–brain barrier and enhance treatment of orthotopic glioma. ACS Appl. Mater. Interfaces 12, 26880–26892. https://doi.org/10.1021/acsami.0c03873.

Griveau, A., Lépinoux-Chambaud, C., Eyer, J., 2021. Effect of the NFL-TBS.40-63 peptide on canine glioblastoma cells. Int. J. Pharm. 605, 120811 https://doi.org/10.1016/j.ijpharm.2021.120811.

Her, S., Jaffray, D.A., Allen, C., 2017. Gold nanoparticles for applications in cancer radiotherapy: Mechanisms and recent advancements. Adv. Drug Deliv. Rev. 109, 84–101. https://doi.org/10.1016/j.addr.2015.12.012.

Heurtault, B., Saulnier, P., Pech, B., Proust, J.E., Benoit, J.P., 2002. A novel phase inversion-based process for the preparation of lipid nanocarriers. Pharm. Res. 19, 875–880. https://doi.org/10.1023/A:1016121319668.

Huang, X., El-Sayed, I.H., Qian, W., El-Sayed, M.A., 2006. Cancer cell imaging and photothermal therapy in the near-infrared region by using gold nanorods. J. Am. Chem. Soc. 128, 2115–2120. https://doi.org/10.1021/ja057254a.

Kreuter, J., 2004. Influence of the surface properties on nanoparticle-mediated transport of drugs to the brain. J. Nanosci. Nanotechnol. 4, 484–488. https://doi.org/10.1166/jnn.2003.077.

Krpetić, Ž., Saleemi, S., Prior, I.A., Sée, V., Qureshi, R., Brust, M., 2011. Negotiation of intracellular membrane barriers by TAT-modified gold nanoparticles. ACS Nano 5, 5195–5201. https://doi.org/10.1021/nn201369k.

Laurin, Y., Savarin, P., Robert, C.H., Takahashi, M., Eyer, J., Prevost, C., Sacquin-Mora, S., 2015. Investigating the structural variability and binding modes of the glioma targeting NFL-TBS.40-63 peptide on tubulin. Biochemistry 54, 3660–3669. https://doi.org/10.1021/acs.biochem.5b00146.

Laurin, Y., Eyer, J., Robert, C.H., Prevost, C., Sacquin-Mora, S., 2017. Mobility and core-protein binding patterns of disordered C-terminal tails in beta-tubulin isotypes. Biochemistry 56, 1746–1756. https://doi.org/10.1021/acs.biochem.6b00988.

Lazär, L.F., Olteanu, E.D., Iuga, R., Burz, C., Achim, M., Clichici, S., Tefas, L.R., Nenu, I., Tudor, D., Baldea, I., Filip, G.A., 2019. Solid lipid nanoparticles: vital characteristics and prospective applications in cancer treatment. Crit. Rev. Ther. Drug Carr. Syst. 36, 537–581. https://doi.org/10.1615/CritRevTherDrugCarrierSyst.2019020396.

Lepinoux-Chambaud, C., Eyer, J., 2013. The NFL-TBS.40-63 anti-glioblastoma peptide enters selectively in glioma cells by endocytosis. Int. J. Pharm. 454, 738–747. https://doi.org/10.1016/j.ijpharm.2013.04.004.

Liu, Q., Aouidat, F., Sacco, P., Marsich, E., Djaker, N., Spadavecchia, J., 2020. Galectin-1 protein modified gold (III)-PEGylated complex-nanoparticles: proof of concept of alternative probe in colorimetric glucose detection. Colloids Surf. B: Biointerfaces 185, 110588. https://doi.org/10.1016/j.colsurfb.2019.110588.

Lo, S.L., Wang, S., 2008. An endosomolytic Tat peptide produced by incorporation of histidine and cysteine residues as a nonviral vector for DNA transfection. Biomaterials 29, 2408–2414. https://doi.org/10.1016/j.biomaterials.2008.01.031.

Malmsten, M., Lindman, B., 1992. Self-assembly in aqueous block copolymer solutions. Macromolecules 25, 5440–5445. https://doi.org/10.1021/ma00046a049.

Margus, H., Arukuusk, P., Langel, Ü., Pooga, M., 2016. Characteristics of cell-penetrating peptide/nucleic acid nanoparticles. Mol. Pharm. 13, 172–179. https://doi.org/10.1021/acs.molpharmaceut.5b00598.

Monteil, M., Moustaoui, H., Picardi, G., Aouidat, F., Djaker, N., de La Chapelle, M.L., Lecouvey, M., Spadavecchia, J., 2018. Polyphosphonate ligands: from synthesis to design of hybrid PEGylated nanoparticles toward phototherapy studies. J. Colloid Interface Sci. 513, 205–213. https://doi.org/10.1016/j.jcis.2017.10.055.

Moustaoui, H., Movia, D., Dupont, N., Bouchemal, N., Casale, S., Djaker, N., Savarin, P., Prina-Mello, A., de la Chapelle, M.L., Spadavecchia, J., 2016. Tunable design of gold (III)–doxorubicin complex–PEGylated nanocarrier. The golden doxorubicin for oncological applications. ACS Appl. Mater. Interfaces 8, 19946–19957. https://doi.org/10.1021/acsami.6b07250.

Naletova, Cucci, D'Angeli, Anfuso, Magrì, La Mendola, Lupo, Satriano, 2019. A tunable nanoplatform of nanogold functionalised with angiogenin peptides for anti-angiogenic therapy of brain tumours. Cancers (Basel). 11, 1322. https://doi.org/10.3390/cancers11091322.

Rivalin, R., Lepinoux-Chambaud, C., Eyer, J., Savagner, F., 2014. The NFL-TBS.40-63 anti-glioblastoma peptide disrupts microtubule and mitochondrial networks in the T98G glioma cell line. PLoS One 9, e98473. https://doi.org/10.1371/journal.pone.0098473.

Schnyder, A., Krähenbühl, S., Drewe, J., Huwyler, J., 2005. Targeting of daunomycin using biotinylated immunoliposomes: Pharmacokinetics, tissue distribution and in vitro pharmacological effects. J. Drug Target. 13, 325–335. https://doi.org/10.1080/10611860500206674.

Shapira, A., Livney, Y.D., Broxterman, H.J., Assaraf, Y.G., 2011. Nanomedicine for targeted cancer therapy: Towards the overcoming of drug resistance. Drug Resist. Updat. 14, 150–163. https://doi.org/10.1016/j.drup.2011.01.003.

Song, S., Gui, L., Feng, Q., Taledaohan, A., Li, Y., Wang, W., Wang, Yanming, Wang, Yuji, 2020. TAT-modified gold nanoparticles enhance the antitumor activity of PAD4 inhibitors. Int. J. Nanomedicine 15, 6659–6671. https://doi.org/10.2147/IJN.S255546.

Spadavecchia, J., Movia, D., Moore, C., Manus Maguire, C., Moustaoui, H., Casale, S., Volkov, Y., Prina-Mello, A., 2016. Targeted polyethylene glycol gold nanoparticles for the treatment of pancreatic cancer: from synthesis to proof-of-concept in vitro studies. Int. J. Nanomedicine 791. https://doi.org/10.2147/IJN.S97476.

Stupp, R., Mason, W.P., van den Bent, M.J., Weller, M., Fisher, B., Taphoorn, M.J., Belanger, K., Brandes, A.A., Marosi, C., Bogdahn, U., Curschmann, J., Janzer, R.C., Ludwin, S.K., Gorlia, T., Allgeier, A., Lacombe, D., Cairncross, J.G., Eisenhauer, E., Mirimanoff, R.O., European Organisation for, R, Treatment of Cancer Brain, T., Radiotherapy, G., National Cancer Institute of Canada Clinical Trials, G, 2005. Radiotherapy plus concomitant and adjuvant temozolomide for glioblastoma. N. Engl. J. Med. 352, 987–996. https://doi.org/10.1056/NEJMoa043330.

Vivès, E., Brodin, P., Lebleu, B., 1997. A truncated HIV-1 tat protein basic domain rapidly translocates through the plasma membrane and accumulates in the cell nucleus. J. Biol. Chem. 272, 16010–16017. https://doi.org/10.1074/jbc.272.25.16010.

Zhu, L., Zhou, Z., Mao, H., Yang, L., 2017. Magnetic nanoparticles for precision oncology: theranostic magnetic iron oxide nanoparticles for image-guided and targeted cancer therapy. Nanomedicine 12, 73–87. https://doi.org/10.2217/nnm-2016-0316.